

Microcavity Length Role On The Characteristic Temperature And The Properties Of Quantum Dot Laser

ISSN -1817 -2695

Ra'ed M. Hassan

Department of Physics, College of Education, University of Basrah, Basrah, IRAQ

Email: raed_m_hassan@yahoo.com

((Received 29/5/2011, Accepted 28/6/2011))

Abstract

Quantum-dot laser devices contains microcavity length which initially populates the properties of quantum dot lasers (QDLs). We studied the influence upon the optical confinement layer free carriers density, confined carrier level occupancies in QDs, threshold current density, internal loss coefficient, characteristic temperature, the maximum operating temperature and QD lowest excitation energy. Our results have been calculated as functions of limit structure parameters of GaInAsP/InP QDL with wavelength of 1.55 μm . The QDL characteristic temperature was studied with the effective cross section and sets an upper limit certain temperature for operating temperature of a QD laser.

Keywords: Quantum dot lasers, microcavity length, characteristic temperature, lowest excitation energy.

1. Introduction

Quantum Dot Laser (QDL) laser devices performance is affected by number of parameters such as; confined electron occupancies, electron threshold current density, modal gain and operation temperature of the device which sought to be near room temperature [1]. There are some of the design elements that plays role controls these parameters (such as cavity length) of QD laser device. By charge neutrality violation studied, the gain and the threshold current are affected strongly on QD laser action [2]. there is also an extra temperature dependence of the gain and threshold current, and introduces the temperature dependence of the electron and hole level occupancies [3,4]. The parasitic recombination outside QDs is fully suppressed, which is the main source of temperature dependence of the modal gain (G_m). Therefore, G_m will still be temperature dependent and characteristic temperature of QD laser (T_0) will remain finite [5]. They are based either on delayed thermal redistribution of the carriers

within QD ensemble on a decrease of the Auger recombination with temperature, or on the increase of homogeneous line-widths of the individual QDs which allows optical coupling between dots [6 - 8].

The carrier density in the optical confinement layer (OCL) is also strongly controlled by the excitation energy from a QD [9]. The smaller excitation energy easier for carriers to escape to OCL depends on the free-electron/hole densities is in the OCL. Just as the characteristic temperature, T_0 exists, there is a lowest excitation energy below which no lasing is attainable in a structure [10]. In this paper, we used rate equations model in steady state of an electrically pumped QD. Our work studies the effected microcavity length of QD laser device on the properties of QDLs such as; confined carrier level occupancies, internal loss coefficient, OCL free-carrier density, QD laser characteristic temperature and QD lowest excitation energy.

2. The Theoretical Model

One can use the rate equations model to calculate the threshold current densities and output powers of longitudinal modes. The steady

state rate equations are used to study carriers confined in QDs, free carriers in the optical confinement layer and photon emission [1]. In

QD laser ideal, the threshold current density (j_{th}) should remain unchanged with temperature and the characteristic temperature T_0 should be infinitely high [11,12]. This would be the case if the overall injection current went into QDs, and the recombination current in QDs would be temperature-independent. In actual QD lasers, carriers are first injected from the cladding layers into the OCL, and then captured into QDs. The presence of carriers in the OCL results in the recombination therein. Hence the recombination processes both in QDs and in the OCL are

$$j_{QDot} = \frac{e \xi_{QDot}}{\tau_{QDot}} f_{QDot}^e f_{QDot}^h, \quad j_{OCL} = e \varphi_{OCL} \mathcal{R}_{OCL} \bar{f}_{OCL}^e \bar{f}_{OCL}^h \quad \dots(1)$$

where $f_{QDot}^{e,h}$ are the confined-electron/hole level occupancies in QDs at the lasing threshold respectively, $\bar{f}_{OCL}^{e,h}$ are the free-electron / hole densities in the OCL at the lasing threshold respectively, ξ_{QDot} is the surface density of QDs, τ_{QDot} is the spontaneous radiative recombination time in QDs, φ_{OCL} is the OCL thickness and \mathcal{R}_{OCL} is the radiative constant for the OCL material.

T -dependence of the confined carrier level occupancies in QDs ($f_{QDot}^{e,h}$) can contribute to different factors, thus causing the temperature-

$$G_m = \frac{\sigma \hbar \Gamma \xi_{QDot}}{4 \mathcal{M}_{QDot} \tau_D \rho (\delta^e E^e + \delta^h E^h)} \left(\frac{\lambda}{\mathcal{L}} \right)^2 \quad \dots(2)$$

where $\delta^{e,h} = -\frac{\partial E^{e,h}}{\partial \ln \mathcal{M}_{QDot}}$, σ is the QD-size distribution function ($\sigma = 1/\sqrt{2\pi}$ for the Gaussian distribution), Γ is the optical confinement factor in the QD layer, ξ_{QDot} is the surface density of QDs, λ is the wavelength of the main mode in vacuum, which is assumed to be the same for all modes, \mathcal{M}_{QDot} is the mean

$$G_m = \frac{\frac{1}{\mathcal{L}} \ln \left[\frac{1}{r} \right] + k_{loss}}{2 f_{QDot}^e - 1} \quad \dots(3)$$

where \mathcal{L} is the cavity length and r is the mirror facet reflectivity. k_{loss} is the overall internal loss coefficient which can be written as the sum of two components: the first is the constant (k_0) and the other is increasing with the OCL electron density (\bar{f}_{OCL}^e), ($k_{loss} = k_0 + \Theta_{ecc} \bar{f}_{OCL}^e$)

controlled j_{th} and its T -dependence [13,14]. The characteristic temperature T_0 has two components; T_0^{QDot} and T_0^{OCL} that defined similarly to T_0 for j_{QDot} and j_{OCL} respectively.

j_{QDot} and j_{OCL} are the components of j_{th} ($= j_{QDot} + j_{OCL}$) associated with the recombination in QDs and in OCL respectively. Those components are given by [13,15]:

dependence of the recombination current density in QDs (j_{QDot}) and making T_0 for j_{QDot} , (T_0^{QDot}) finite [6,16].

In addition to free-carrier absorption in the OCL and scattering at rough surfaces and imperfections in the waveguide [17], several mechanisms can contribute to the internal loss. All these mechanisms can be conveniently grouped into two categories – one dependent on the carrier density in the OCL and the others are not. The expression for the maximum (saturation) value of the modal gain G_m is [13]

size of QDs, ρ is RMS of relative QD-size fluctuations, $E^{e,h}$ are the electron /hole quantized energy levels in a mean-sized QD (measured from the corresponding band edges) [2] and \mathcal{L} is the group index of the dispersive OCL material.

The lasing threshold condition (equality of the gain to the loss) can be written as [18];

[14,17], where Θ_{ecc} is the effective cross section for the internal absorption loss processes.

The level occupancy is immediately obtained from Eq.(2) to be independent of temperature, in the absence of the electron-density-dependent internal loss ($\Theta_{ecc} = 0$) [9];

$$f_{QDot}^e = \frac{1}{2} \left[1 + \frac{k_0 + \mathcal{R}_{loss}}{G_m} \right] \quad \dots(4)$$

where f_{QDot}^e are the confined-electron level occupancies in QDs at the lasing threshold ($f_{QDot}^e = f_{QDot_0}^e$ at $\theta_{ecs} = 0$), The electron-density-dependent internal loss couples f_{OCL}^e and f_{QDot}^e , as seen from Eq.(2), makes f_{QDot}^e and

$$f_{QDot}^e = \frac{1}{2}(1 + f_{QDot_0}^e - W) - \sqrt{\frac{1}{4}(1 + f_{QDot_0}^e - W)^2 - f_{QDot_0}^e} \quad \dots(5)$$

where $W = f_{OCL_0}^e \frac{\theta_{ecs}}{2G_m}$. Affecting the characteristic temperature T_0 via its effect on the level occupancy f_{QDot}^e , due to the carrier-density-dependent internal loss formally plays a role similar to that violation of charge neutrality in QDs [15,18].

The expression for the characteristic temperature component T_0^{QDot} yields the following [9,10];

$$\frac{1}{T_0^{QDot}} = \frac{\frac{W}{T} \left(3 + \frac{2\varepsilon^e}{T}\right)}{\sqrt{(1 + f_{QDot_0}^e - W)^2 - 4f_{QDot_0}^e}} \quad \dots(6)$$

At the lasing threshold, the free-carrier density is strongly effective therefore carrier-density-dependent internal loss also alters the temperature dependence of J_{OCL} . The expression for T_0^{OCL} in this case [14];

$$\frac{1}{T_0^{OCL}} = \frac{1}{2} \left[\frac{3}{T} + \frac{4\varepsilon^e}{T^2} + \frac{2}{T_0^{QDot}(1 - f_{QDot}^e)} \right] \quad \dots(7)$$

The position effect of characteristic temperature from the critical point is important to determine the QD laser operation [13].

$$1/T_0 = \left(\frac{J_{QDot} + J_{OCL}}{T_0^{QDot} + T_0^{OCL}} \right) / j_{th} \quad \dots(8)$$

The carrier distribution below and at the lasing threshold is described by the equilibrium statistics (relatively high T). Thus, the T -dependence of free-carrier densities ($f_{OCL}^{e,h}$) have acts as the major source of such dependence of J_{th} [15-17] as follows [17];

3. The results and discussion

In this work, we used a GaInAsP/InP QDL with 1.55 μm wavelength for calculations modal gain dependent cavity length of QD laser device. By using Eq. (1), that shows the results of the

J_{QDot} also temperature dependent in view of the temperature dependence of f_{OCL}^e . Thus, T_0^{QDot} becomes finite. The expression for f_{QDot}^e was derived in Ref.[17];

$$f_{OCL}^{e,h} = 2 \left(\frac{m_{OCL}^{e,h} T}{2\pi\hbar^2} \right)^{3/2} e^{-\frac{\varepsilon^{e,h}}{T}} \frac{f_{QDot}^{e,h}}{1 - f_{QDot}^{e,h}} \quad \dots(9)$$

where $m_{OCL}^{e,h}$ are the electron/ hole effective masses in the OCL respectively, T is the temperature measured in units of energy, $\varepsilon^{e,h}$ are the electron/hole excitation energies from a QD to the OCL.

The carrier density f_{OCL}^e in the OCL is also strongly controlled by the excitation energy E^e from a QD. To the OCL with smaller E_e , higher f_{QDot}^e and k_{loss} is easier for carriers to escape [10]. With no lasing attainable in the structure, there is a lowest excitation energy E_{low}^e [9];

$$E_{low}^e = T \ln \left[\frac{2 \theta_{ecs} \left(\frac{m_{OCL}^e T}{2\pi\hbar^2} \right)^{3/2}}{\left(\sqrt{2G_m} - \sqrt{G_m + k_{loss}} + \frac{1}{\zeta} \ln \left[\frac{1}{r} \right] \right)^2} \right] \quad \dots(10)$$

The thermal escapes from QDs to the OCL will be so intensive. So that the population inversion required for the lasing cannot be attained [6]. With reducing QD size, there is also exists a smallest tolerable QD size since E^e decreases [10]. A more strict condition should be satisfied to attain lasing in the presence of the microcavity length-dependent [9].

theory of the impact of cavity length, \mathcal{L} on the relationship between the threshold current density, J_{th} and OCL component J_{OCL} against

temperature, T which appears exponential. As shown in Fig. 1, we can note that increasing \mathcal{L} is working to reduce the j_{th} with making the QD microcavity maximum operating temperature within the long range.

OCL threshold current density component, j_{OCL} has a lower curve with the temperature, but with the least amount. That addition to the amount of j_{th} comes from the QD threshold current density component, j_{QDot} . The curves end in both cases at the same maximum operating temperature. The inclined dashed line

in the figure shows a positive linear relationship between the two axes of the characteristic temperature, T_0 and j_{th} of the impact of increasing the length of the cavity.

Fig. 2 shows the temperature dependence of internal loss coefficient, k_{loss} , which increased exponentially until it reaches T_0 similar to the behavior in the Fig. 1. The effect of increasing the cavity length on maximum operating temperature properties and k_{loss} is similar to Fig. 1.

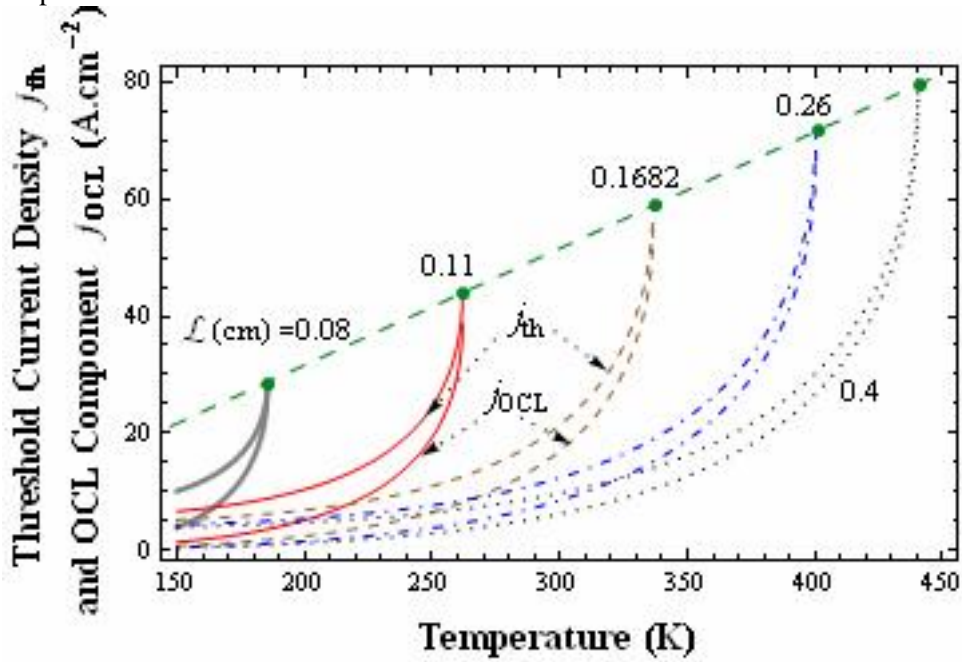


Figure 1: Threshold current density, j_{th} and OCL component, j_{OCL} vs. temperature, T from Eq.(1) for different value of cavity length; \mathcal{L} (cm) = 0.08, 0.11, 0.1682, 0.26 and 0.4. The straight line marks the QD microcavity maximum operating temperature in the presence of the carrier density dependent internal loss. The parameters used for GaInAsP/InP QDL with 1.55 μm wavelength [10]: $\Gamma = 0.01$, $\xi_{QDot} = 6.11 \times 10^{10} \text{ cm}^{-2}$, $\lambda = 1.55 \mu\text{m}$, $\mathcal{M}_{QDot} = 150 \text{ A}^\circ$,

$$E^g = 6. \text{ meV}, \rho = 0.05, r = 0.32, k_{loss} = 3. \text{ cm}^{-1} \text{ and } \theta_{ecc} = 2.67 \times 10^{-17} \text{ cm}^2.$$

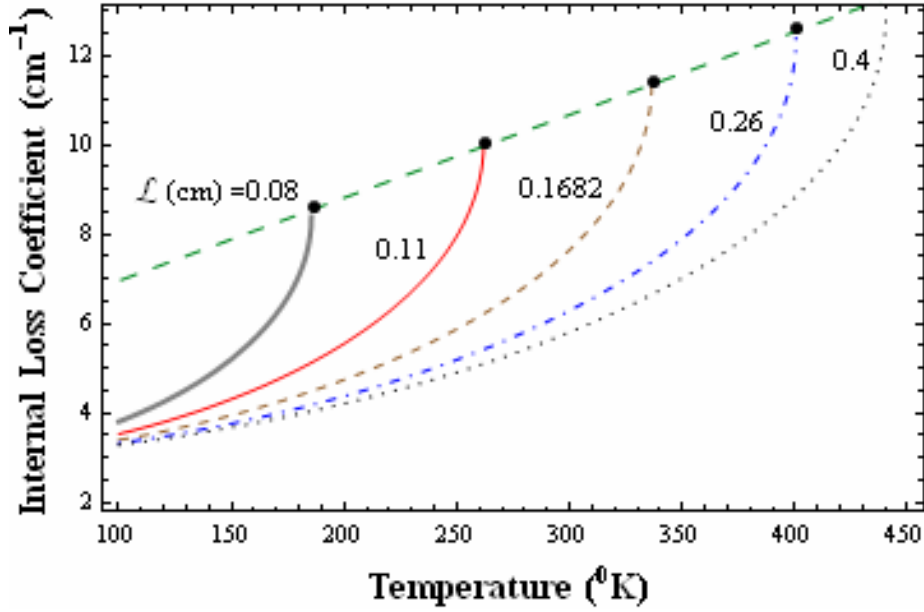


Figure 2: Internal loss coefficient, k_{loss} vs. temperature, T ; for different value of cavity length; \mathcal{L} (cm) = 0.08, 0.11, 0.1682, 0.26 and 0.4. The straight line marks the QD microcavity maximum operating temperature. The parameters used are such as in Fig. 1.

The situation is reversed with temperature dependence of confined-electron occupancies QDs, the behavior remains the same where it is increased exponentially. Also the case with the T_0 in Fig. 3. But the increase of the cavity length works to increase the value of confined-electron occupancies and reduction maximum operating temperature. So the slope of the straight line in Fig. 3, which represents the maximum operating temperature against temperature has a negative amount. This means that the increase in the determination of QD laser design in the operation temperature range. That the impact of the \mathcal{L} change on the characteristic temperature of QD, T_0^{QDot} and OCL, T_0^{OCL} is shown in Fig. 4. We can find the T_0^{QDot} curves have high values at low temperature, which falls with increasing T to zero when the amount of T depends on the \mathcal{L} . While, T_0^{OCL} starts at much lower values of temperature which increases relatively low, then it land until it reaches zero at the same temperature as T_0^{QDot} .

Our theoretical study contains the relationship of T_0 against \mathcal{L} with a more detailed manner with the presence or the absence of the effective cross-section as shown in Fig. 5. In this figure, we find that the presence of the effective cross-section begins from zero in certain \mathcal{L} . The

curves increase rapidly, then that tends to stabilize at the long range of length. But in the absence of the effective cross-section, all the curves have specific values of T_0 when \mathcal{L} is small. However, that behaves are start to increase with increasing the cavity length until it reaches specific amount in a longer-large of \mathcal{L} . In Fig. 5(a), note the impact increased of RMS of relative QD-size fluctuations, ρ works on necessity increasing \mathcal{L} to start laser action reducing T_0 . The impact of this factor is greater in the case of effective cross-section is present. Fig. 5(b) shows the role played by a mirror facet reflectivity; r on the device characteristics. By increasing this factor, it leads for a shorter \mathcal{L} . Any shorter length can be used to reach T_0 of the specific properties of QD laser. The impact of the mean size of QDs; \mathcal{M}_{QDot} observed in Fig. 5(c), which characterizes this factor as a attenuation factor to the QD lasing characteristics. So, the increase of this factor required to increase \mathcal{L} to get the QD laser action and it reduces the T_0 . While the situation is reflected with the increase of the surface density of QDs; ξ_{QDot} is effective in reducing the need for large \mathcal{L} as shown in Fig. 5(d).

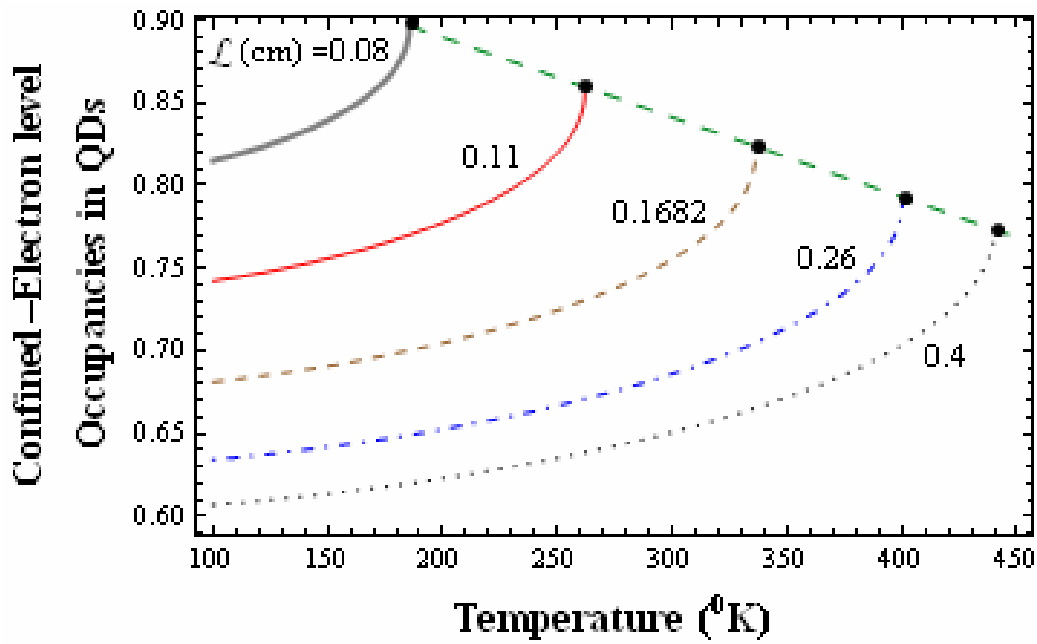


Figure 3: Confined-carrier level occupancy in QDs, f_{QDot}^e vs. temperature, T from Eq.(5); for different value of cavity length; \mathcal{L} (cm) = 0.08, 0.11, 0.1682, 0.26 and 0.4.

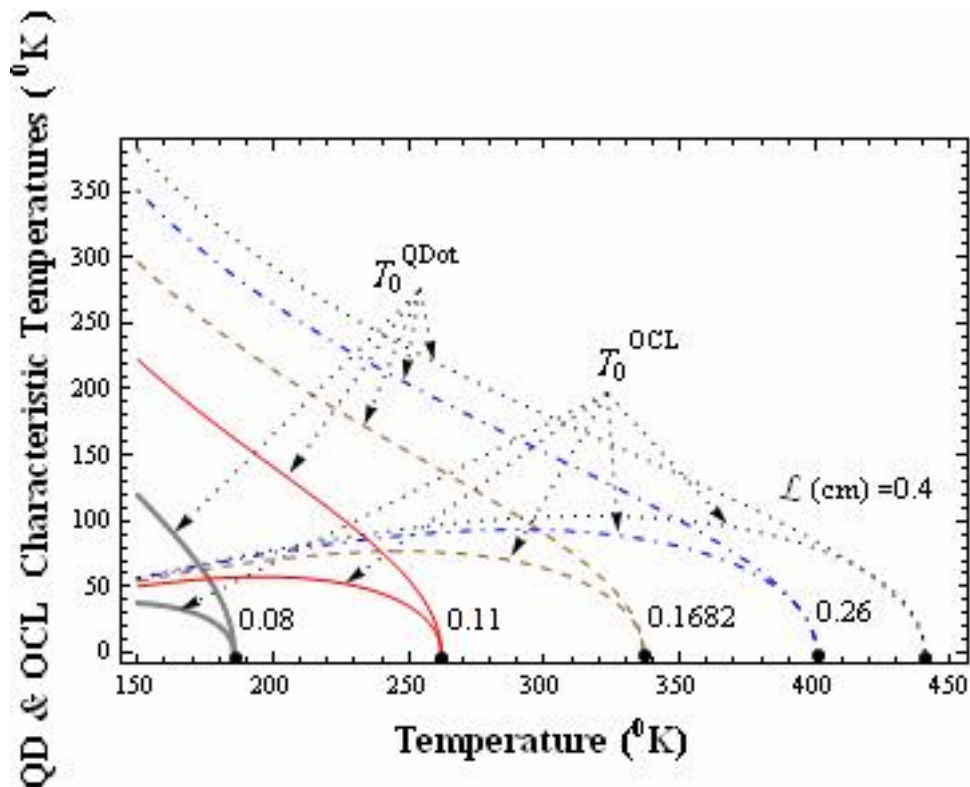


Figure 4: QD and OCL characteristic temperature vs. temperature, T from Eqs.(6) & (7); for different value of cavity length; \mathcal{L} (cm) = 0.08, 0.11, 0.1682, 0.26 and 0.4.

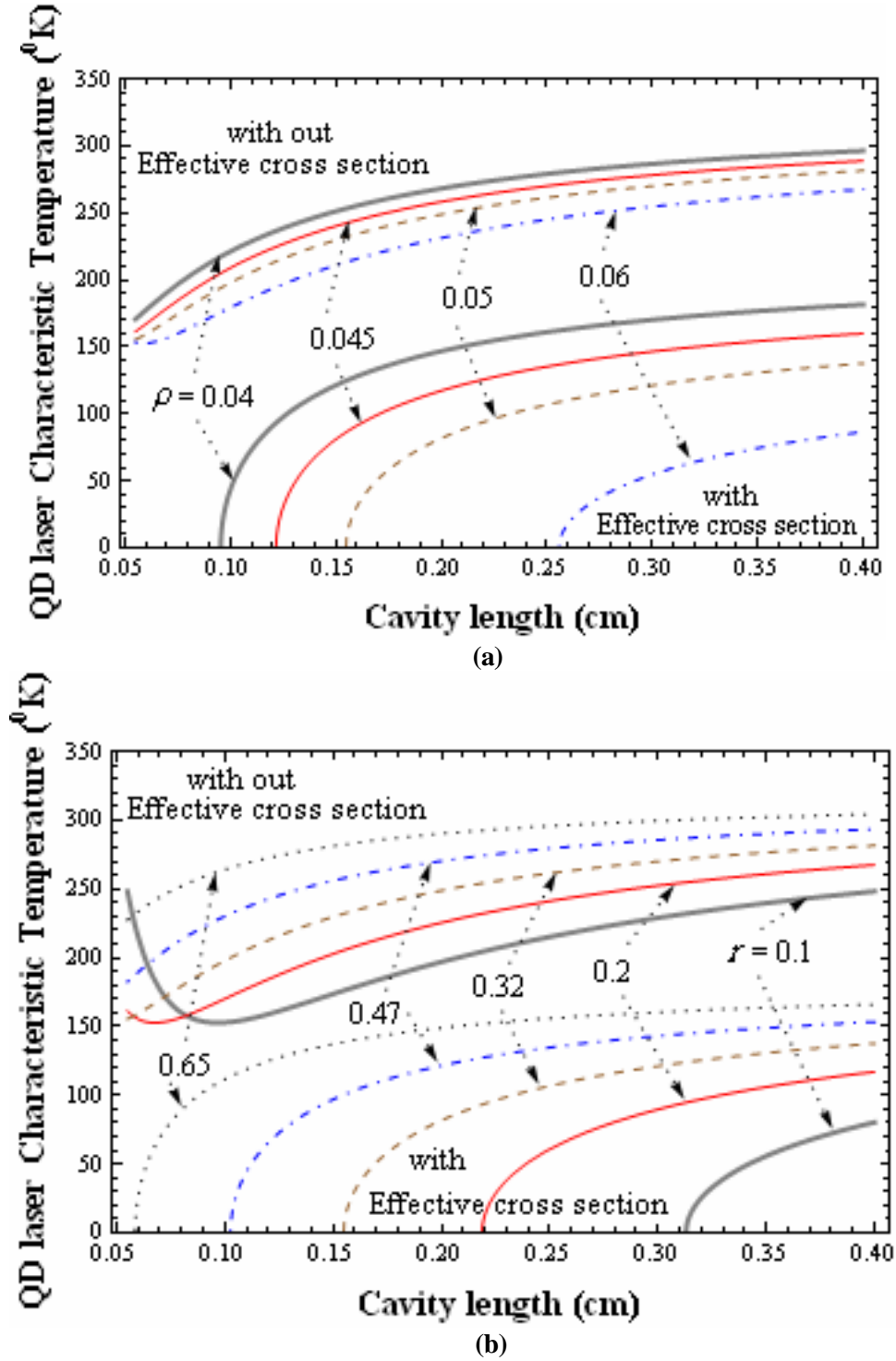


Figure 5: Laser Characteristic Temperature, T_0 vs. cavity length, L from Eq.(8) for different value of; (a) RMS of relative QD-size fluctuations; $\rho = 0.04, 0.045, 0.05$ and 0.06 respectively, (b) Mirror facet reflectivity; $r = 0.1, 0.2, 0.32, 0.47$ and 0.65 respectively, (c) Mean size of QDs; $M_{QDot}(\text{\AA}) = 120, 135, 150, 180$ and 200 respectively, and (d) Surface density of QDs; $\xi_{QDot}(\times 10^{10} \text{ cm}^{-2}) = 5.3, 6.11, 6.9$ and 7.7 . The above/below curves indicates T_0 in the absence/presence of the carrier-density-dependent internal loss (effective cross section for the internal absorption loss processes) respectively.

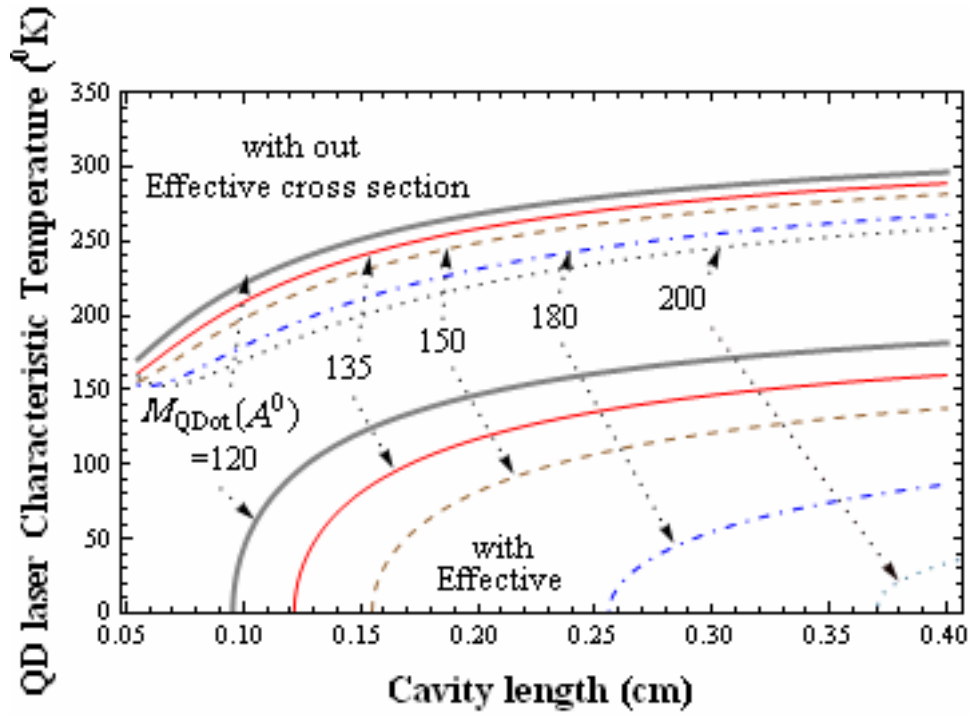


Figure 5: (c)

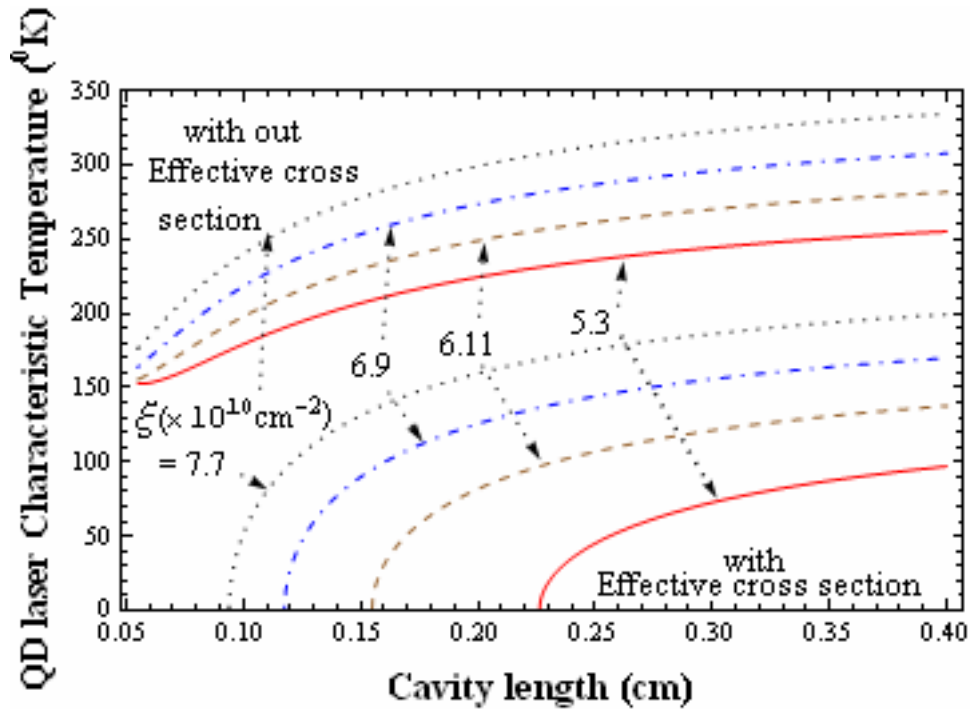


Figure 5: (d)

The effect of OCL free-electron density, f_{ocL}^e included is described in Fig. 6. The conduct of the relationship in this figure is similar to the situation in Fig. 2. We find the effect of increasing \mathcal{L} leads to increase the amount of the OCL free-electron density with T_0 be in far range. Therefore, we can find that the slope of the QD microcavity maximum operating temperature is shown as a positive tendency.

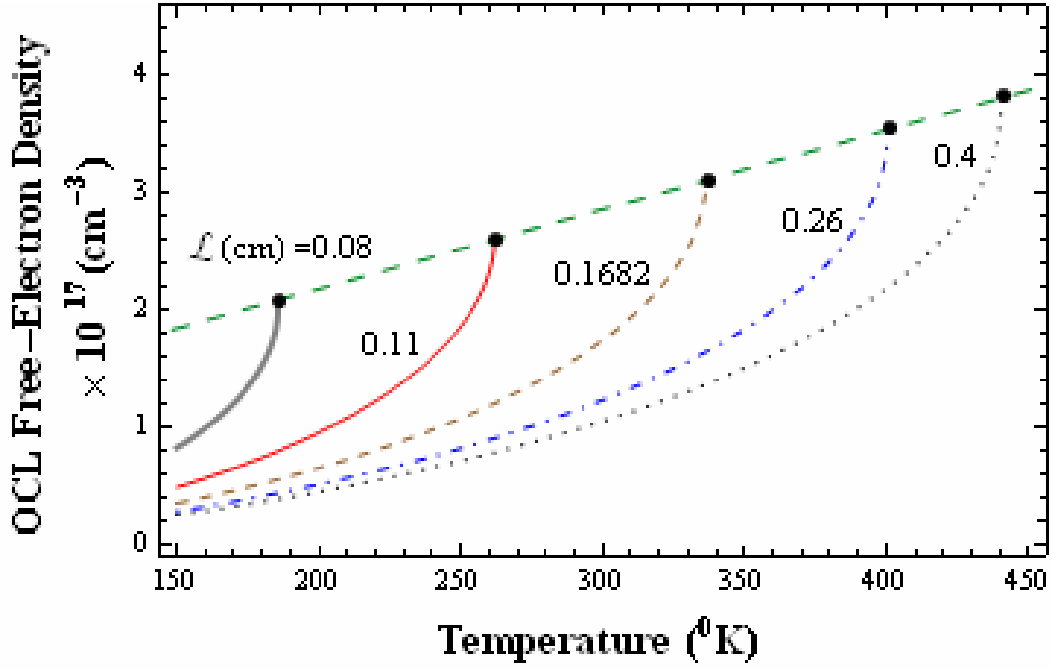
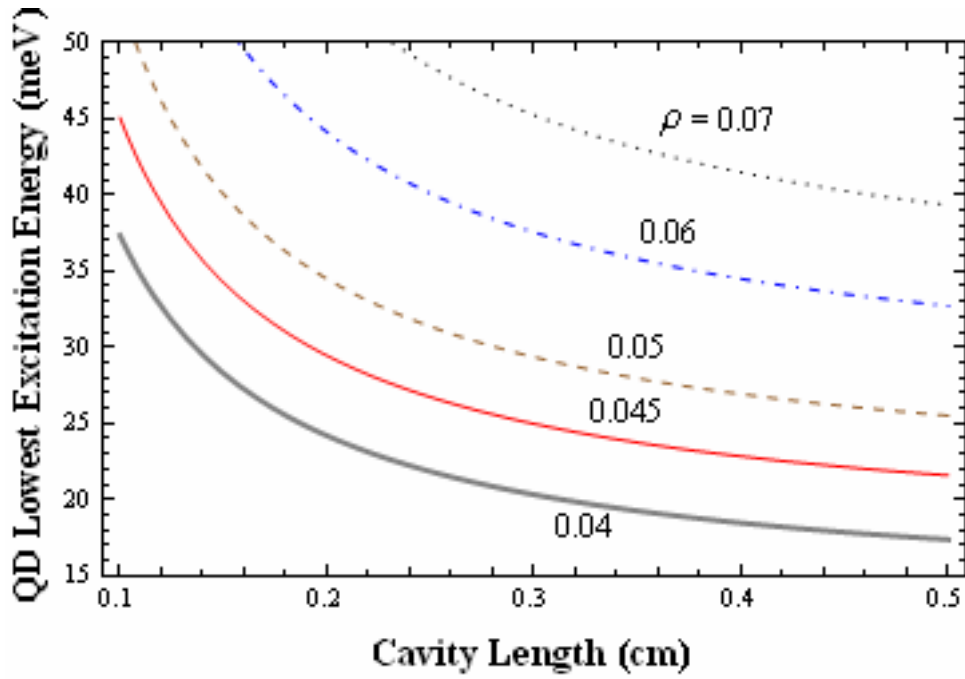


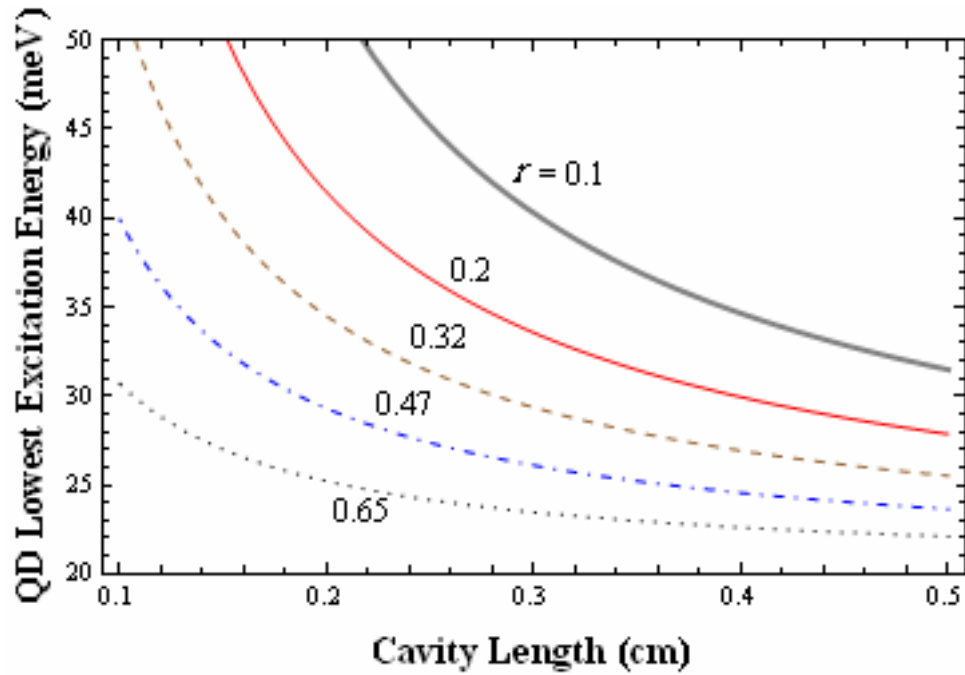
Figure 6: OCL free-electron density, f_{ocl}^e vs. temperature, T from Eq.(9) for different value of cavity length; \mathcal{L} (cm) = 0.08, 0.11, 0.1682, 0.26 and 0.4. The straight line marks the QD microcavity maximum operating temperature.

One of the most important aspects which the designer seeks to know in QD laser device, is the amount of QD lowest excitation energy, E_{low}^e . This is what we have studied in Fig. 7 with studying the effect of four control parameters which are shown in Fig. 5. In Fig. 7, we can find that the negative exponential relationship with increasing \mathcal{L} . There are negative exponential curves between increasing \mathcal{L} is accompanied by an exponential decline of E_{low}^e (less QD lowest excitation energy). Fig. 7(a) shows the effect of ρ , that any increase in this factor tends to increase E_{low}^e . Here, that requires a significant increase in the \mathcal{L} to reduce the amount of E_{low}^e . An increase in r has an

important role which is evident in Fig. 5(b), that is repeated in Fig. 7(b) which works to reduce E_{low}^e so as it provide to shorten \mathcal{L} effect to create a QD laser action. In Fig. 7(c), we can find through the impact of changing \mathcal{M}_{QDot} that has a negative impact on increasing the amount of E_{low}^e . Therefore with a large \mathcal{M}_{QDot} that is need to large E_{low}^e . While it is very different from the role of increased ξ_{QDot} as shown in Fig. 7(d), with an increase of this important factor that will lead to reduce of the E_{low}^e . So that will lead to savings in the amount of \mathcal{L} which necessary to QD microcavity lasing.



(a)



(b)

Figure 7: QD lowest excitation energy, E_{low}^e vs. cavity length, \mathcal{L} from Eq.(10) for different value of; (a) RMS of relative QD-size fluctuations; $\rho = 0.04, 0.045, 0.05, 0.06$ and 0.07 respectively, (b) Mirror facet reflectivity; $r = 0.1, 0.2, 0.32, 0.47$ and 0.65 respectively, (c) Mean size of QDs; $\mathcal{M}_{QDot} (\text{\AA}^n) = 120, 135, 150, 180$ and 200 respectively, and (d) Surface density of QDs; $\xi_{QDot} (\times 10^{10} \text{ cm}^{-2}) = 4.5, 5.3, 6.11, 6.9$ and 7.7 .

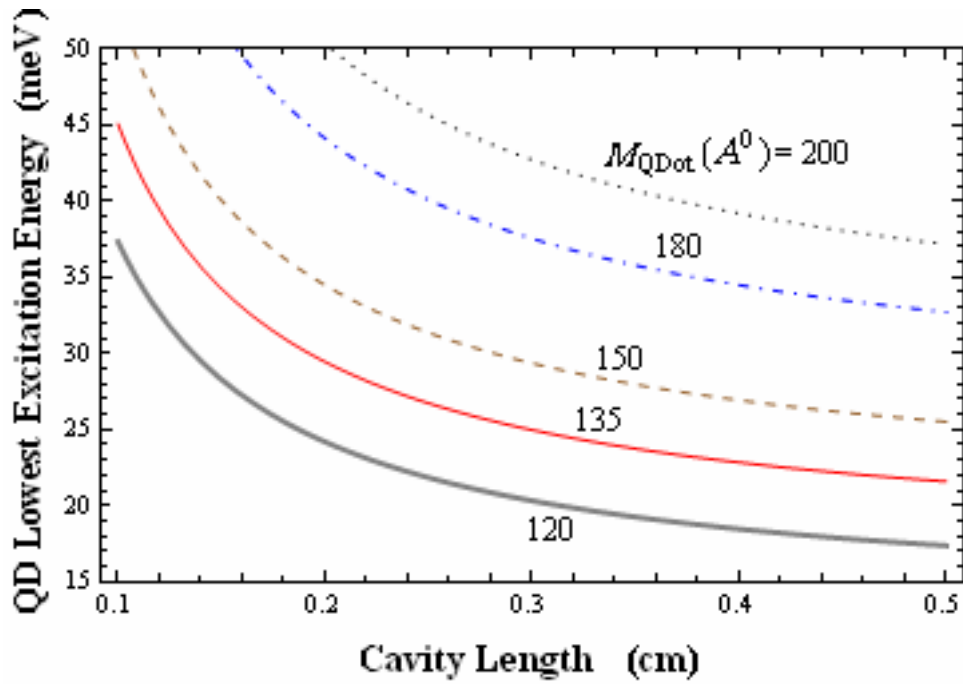


Figure 7: (c)

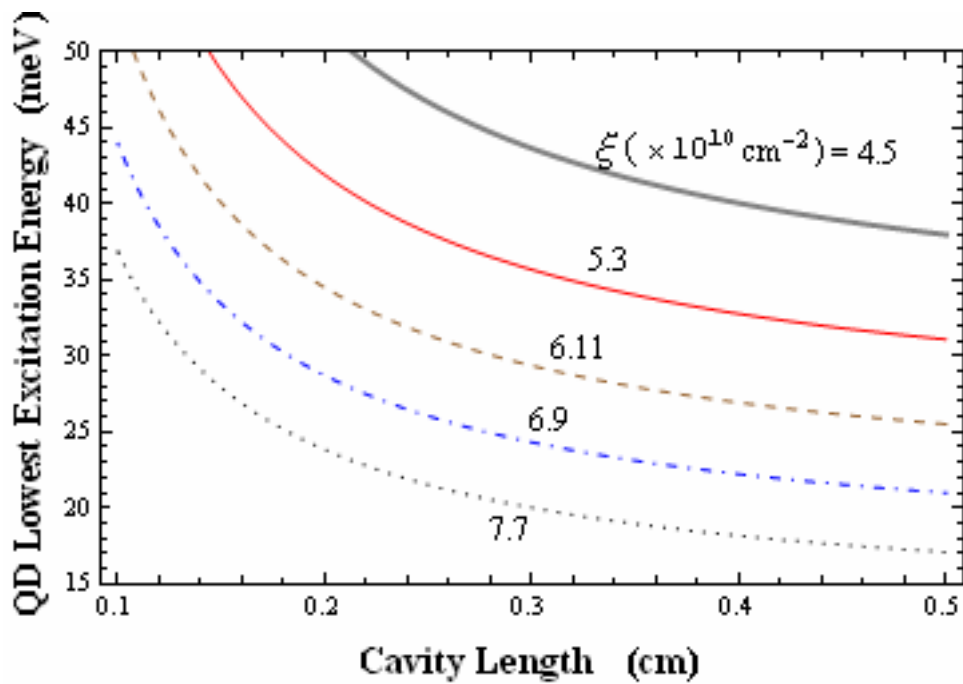


Figure 7: (d)

4. Conclusion

It is imposed for the QDL designer to determine the cavity length in the range of relatively short lengths which is reflected on the characteristics of QD laser. From our theoretical results in this paper, we found that with the reduction of the microcavity length is reflected negatively to increase the threshold current density, the internal losses coefficient, and QD and OCL an characteristic temperature, while,

that reduces the confined-carrier level occupancy in QDs. One can be remedied this problem by reducing the RMS of relative QD-size fluctuations and the mean size of QDs or increase of the mirror facet reflectivity and the surface density of QDs. Also it is useful to know the impact of this factor on the QD lowest excitation energy. So we found that reducing of

the microcavity length is working to reduce this energy.

References

- [1] T. Steiner. "Semiconductor Nanostructures for Optoelectronic Applications". © ARTECH HOUSE, INC., (2004).
- [2] L. V. Asryan, M. Grundmann, Nikolai N. Ledentsov, Oliver Stier, Robert A. Suris, and Dieter Bimberg. IEEE Journal of Quantum Electronics, 37(3):418-425, (2001).
- [3] I. O'Driscoll, P. Blood, and P. M. Smowton. IEEE Journal of Quantum Electronics, 46(4): 525-532, (2010).
- [4] S. G. Li, Q. Gong, Y.F. Lao, Y.G. Zhang, S.L. Feng, and H.L. Wang. Electronics Letters, 46(2): 158 - 159, (2010).
- [5] P. F. Xu, T. Yang, H. M. Ji, Y. L. Cao, Y. X. Gu, Y. Liu, W. Q. Ma, and Z. G. Wang. Journal of Applied Physics, 107: 013102(1-5), (2010).
- [6] D. S. Han and L. V. Asryan. IEEE Journal of Lightwave Technology, 27(24):5775- 5782, (2009)
- [7] I. Alghoraibi, T. Rohel, R. Piron, N. Bertru, C. Paranthoen, G. Elias, A. Nakkar, H. Folliot, A. Le Corre, and S. Loualiche. Applied Physics Letters, 91: 261105(1-3), (2007).
- [8] I. Alghoraibi, T. Rohel, R. Piron, N. Bertru, C. Paranthoen, G. Elias, A. Nakkar, H. Folliot, A. Le Corre, S. Loualiche.. IEEE Information and Communication Technologies: Form Theory to Applications, 3rd International Conference on, 10053311(1-5), (2008).
- [9] L. Jiang. PhD. thesis, Virginia Polytechnic Institute and State University, USA, (2008).
- [10] L. Jiang and L.V. Asryan. Laser Physics Letters, 4(4): 265–269, (2007).
- [11] Y. Arakawa and H. Sakaki, Applied Physics Letters, 40(11): 939–941, (1982).
- [12] K. Akahane, N. Yamamoto, and T. Kawanishi. IEEE Photonics Technology Letters, 22(2): 103-105, (2010).
- [13] L. V. Asryan and R. A. Suris. Semicond. Sci. Technol., 11(4): 554–567, (1996).
- [14] R. M. Hassan, C. A. Emsary, S. I. Easa. " Turn-on Carrier Excitation Energies from a QD to OCL, RMS of Relative QD-Size Fluctuations and Temperature Dependence of QDL". Journal of Thi-Qar Science, (to be published).
- [15] L. V. Asryan and R. A. Suris. IEEE Journal of Quantum Electronics, 34 (5): 841-850, (1998).
- [16] D. S. Han and L. V. Asryan. Solid-State Electronics, 52: 1674–1679, (2008).
- [17] L.V. Asryan and S. Luryi. IEEE Journal of Quantum Electronics, 40(7): 833-843, (2004).
- [18] L. V. Asryan and R. A. Suris. IEEE Journal of Selected Topics in Quantum Electronics, 3(2):148-157, (1997).

دور طول التجويف المايكروفي في درجة حرارة الخاصية و مميزات ليزر النقطة الكمية

رائد محمد حسن

قسم الفيزياء، كلية التربية، جامعة البصرة، البصرة - العراق

الخلاصة:

أجهزة ليزر النقطة الكمية (QD) تحتوي على طول التجويف المايكروفي الذي هو أبتداءا يقوم بتأهيل خصائص ليزرات النقطة الكمية (QDLs). دراسنا هذا التأثير على كثافة الحاملات الحرة لطبقة الحجز البصري ، الإشغال مستوى الحامل المقيد في QDs ، وكثافة تيار العتبة ، معامل الخسارة الداخلية ، درجة الحرارة الخاصية ، درجة حرارة التشغيل القصوى و الطاقة التهييج أدنى للـ QD. حسبنا نتائجنا كدالة لبرامترات تركيب محددة للـ QDL نوع GalnAsP /InP عند الطول الموجي 1.55ميكرومتر . كما درست درجة الحرارة خصائص QDL مع المقطع العرضي الفعال ومجموعات لحدود أعلى من درجة حرارة المؤكدة لدرجات حرارة التشغيل ليزر QD.